NJC

ROYAL SOCIETY OF CHEMISTRY

PAPER

View Article Online
View Journal | View Issue

Cite this: *New J. Chem.*, 2024, **48**, 13900

One-pot preparation of pyrazole "turn on" and "turn off" fluorescent sensors for Zn^{2+} and Cd^{2+} directly from chalcones *via in situ* aromatisation†

Alexander Ciupa

Received 25th May 2024,
Accepted 11th July 2024

DOI: 10.1039/d4nj02433h

rsc.li/njc

A direct chalcone to pyrazole synthetic route to "turn on" and "turn off" fluorescent sensors for Cd^{2+} and Zn^{2+} was developed using $CuCl_2$ as an *in situ* oxidant. This one-pot approach produced eight novel pyridine based pyrazole fluorescent sensors displaying both "turn on" and "turn off" properties dependent on the substutient on the aryl ring (4-F, 4-Cl, 4-Br, 4-I, 4-CN, 4-NO_2, 4-OMe and 3,4-OMe). The results within provide valuable insight for future pyrazole sensor design.

Introduction

Pyrazole,[1] a five-membered heterocycle with two adjacent nitrogen atoms (red in Fig. 1), is a privileged structure[2] with a diverse range of biological activities including anti-inflammatory,[3] anti-cancer[4] and anti-infective[5] properties. 3,5 substituted pyrazoles have unique photophysical properties with applications in luminescent dyes[6] and fluorescent sensors.[7] "Turn off" fluorescent sensors display reductions in fluorescent emission (λ_{em}) with analyte, for example **1** with picric acid[8] and **2** with Cu^{2+} and Ni^{2+} (Fig. 1).[9] "Turn on" fluorescent sensors are characterised by increased λ_{em} with analyte, **3** demonstrates Fe^{3+}/Fe^{2+} selectivity[10] and **P1** displays a "turn on" response with Zn^{2+} and Cd^{2+} in MeCN (Fig. 1).[11]

Zinc is involved in a variety of biological functions including gene expression,[12] enzyme maintenance[13] and neurological functions.[14] Cadmium, also a group 12 element sitting below zinc in the periodic table, is a highly toxic pollutant implicated in a variety of cancers.[15] **3** and **P1** demonstrate structural complexity is not a prerequisite for complex functionality and that simple molecular structures can detect biologically important analytes.[10,11]

Chalcones,[16] also a privileged structure with numerous biological activities,[17] are popular precursors for pyrazoles due to the range of inexpensive commercially available starting materials. To date, there are few examples of direct chalcone to pyrazole syntheses, often requiring vigorous heating under acidic conditions[18] or use of a catalyst.[19] The traditional two step synthesis involves 1,2 addition of hydrazine to the enone[10,11,20] forming a pyrazoline[21] which is isolated, purified, and undergoes subsequent aromatisation to a pyrazole (blue and red respectively (Scheme 1).

A range of chemical oxidants have been reported to perform this pyrazoline to pyrazole aromatisation including MnO_2,[22] $FeCl_3$,[23] $CoCl_2$[24] and $CuCl_2$.[25] Previous work[10] demonstrated the addition of 8.0 equivalents (eq.) methylhydrazine at room temperature resulted in minor formation of pyrazole (yield 8–18%). Herein we report optimisation of this reaction enabling efficient access to the pyrazole privileged structure directly from chalcone avoiding the requirement to isolate, purify and then aromatise the pyrazoline ring separately. We examined multiple reaction conditions and screened eight different transition metal oxidants. Direct one-pot access to pyrazole sensors facilitated rapid synthesis and screening of eight novel Zn^{2+} and Cd^{2+} "turn on" and "turn off" pyrazole sensors.

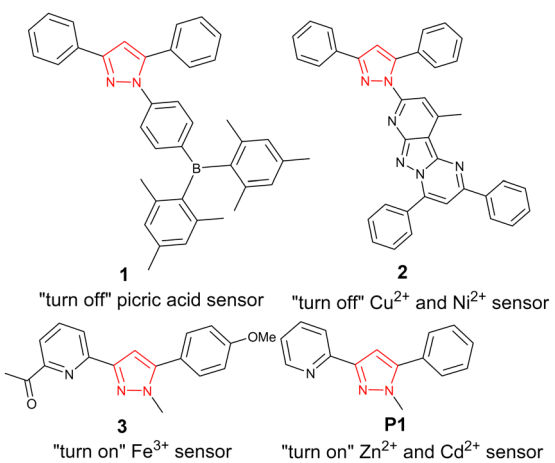

Fig. 1 A selection of 3,5 substituted "turn off" and "turn on" sensors.

Materials Innovation Factory, University of Liverpool, 51 Oxford Street, Liverpool L7 3NY, UK. E-mail: ciupa@liverpool.ac.uk

† Electronic supplementary information (ESI) available. See DOI: https://doi.org/10.1039/d4nj02433h

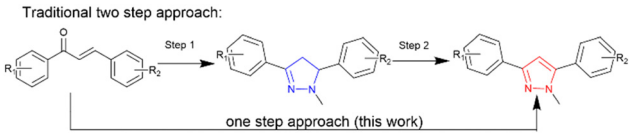

Scheme 1 A one step approach to synthesise pyrazole (in red) directly from chalcone avoiding the pyrazoline (in blue) intermediate step.

Results and discussion

Chalcone **C1** is the precursor for **P1** and was selected as a model system for reaction screening (Scheme 2).

Previous work[10] was used as a baseline (entry 1, Table 1) and ^{1}H NMR was used to determine the percentage (%) conversion of **C1** to **P1** using the ratio of the chemically distinct methyl (CH_3) groups in the pyrazoline **P1*** at approx. 2.90 ppm and the pyrazole methyl (CH_3) at approx. 4.30 ppm (shown in blue and red in Fig. 2, see ESI† for full study).

Preliminary conditions produced 18% conversion of **C1** to **P1** with pyrazoline **P1*** the residual component (Table 1). Solvent, consisting of the bulk of the reaction mixture, was initially screened using a variety of polar/nonpolar and protic/nonprotic solvents.

Polar protic solvents MeOH, EtOH and iPrOH (entries 1–3, Table 1) were initially investigated with MeOH providing the best % conversion of 18%. Polar aprotic solvents (MeCN and THF, entry 4 and 5, Table 1) reduced % conversion to 11% and 7% respectively. Chlorinated solvents CH_2Cl_2 and $CHCl_3$ (entries 6 and 7, Table 1) failed to provide an improvement with 10% and 13% **P1** conversion. Interestingly the use of the nonpolar aprotic solvent hexane was highly detrimental to **P1** formation with 98% conversion to **P1*** and only 2% **P1** (entry 8, Table 1). Hexane would be an excellent choice for pyrazoline only targeted synthesis. Eight solvents were screened and the preferred solvent for pyrazole formation was MeOH, this was fixed and used for all subsequent reactions. The reaction temperature was varied to 40 °C and then 60 °C with a further improvement on **P1**% conversion to 30% and 40% respectively (entry 9 and 10, Table 1). The temperature was fixed at 60 °C to provide the best **P1** conversion while remaining below both the boiling points of MeOH and methylhydrazine (H_2NNHMe). The number of equivalents (eq.) H_2NNHMe was varied, surprisingly reducing the eq. of H_2NNHMe to 2.0 did not significantly reduce the **P1**% conversion (entry 12, Table 1). Further increases in eq. H_2NNHMe did not yield an improvement therefore according to the principle of atom efficiency and green chemistry[26] 2.0 eq. H_2NNHMe was used for all further reactions.

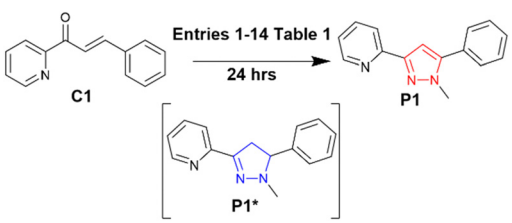

Scheme 2 Preliminary reaction condition screening.

Table 1 Preliminary reaction condition screening for pyrazole **P1**, % conversion determined by ^{1}H NMR from duplicate experiments (see ESI). Bold indicates the optimum selection per parameter

Entry	Solvent	Temperature (°C)	Eq. H_2NNHMe	**P1** % conversion
1	**MeOH**	20	8.0	18
2	EtOH	20	8.0	10
3	iPrOH	20	8.0	3
4	MeCN	20	8.0	11
5	THF	20	8.0	7
6	CH_2Cl_2	20	8.0	10
7	$CHCl_3$	20	8.0	13
8	Hexane	20	8.0	2
9	MeOH	40	8.0	30
10	MeOH	**60**	8.0	40
11	MeOH	60	1.5	38
12	MeOH	60	**2.0**	40
13	MeOH	60	4.0	35
14	MeOH	60	16	32

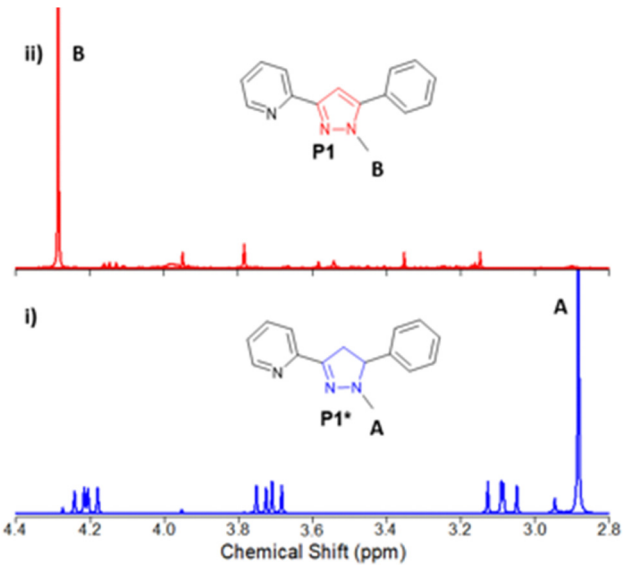

Fig. 2 Representative example of ^{1}H NMR study to determine the % conversion of methyl group A in **P1*** (in blue, entry 18, Table 2, i) to methyl group B in **P1** (in red, entry 19, Table 2, ii).

The initial reaction condition optimisation (Table 1) resulted in a significant increase in **P1** pyrazole formation from 18% to 40%, we then investigated if the presence of an oxidant would improve the *in situ* aromatisation of the pyrazoline to a pyrazole (Scheme 3 and Table 2).

MnO_2 has been reported to be a useful oxidant for pyrazole formation[22] however it reduced conversion to 25% (entry 15, Table 2). A similar effect was observed with $FeCl_3$, $CoCl_2$ with the presence of 1.0 eq. $NiCl_2$ highly detrimental to pyrazole formation (entries 16–18, Table 2). 1.0 eq. $ZnCl_2$ produced a slight increase in conversion to 45% (entry 20, Table 2) however the addition of $CuCl_2$ was the most promising with a more than doubling of conversion to 83% (entry 19, Table 2). Encouraged by this result, we investigated two different copper salts, $CuSO_4$ and $Cu(OAc)_2$ which yielded 64% and 78% conversion

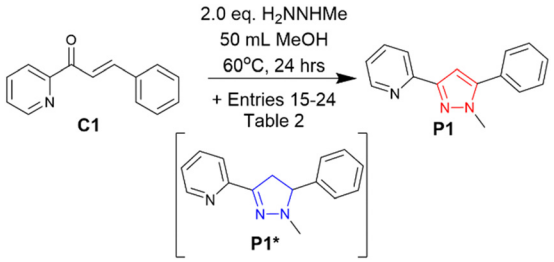

Scheme 3 Oxidant screening.

Table 2 *In situ* oxidant screening for **P1** using the optimum conditions from entry 12, Table 2 (2 eq. H_2NNHMe, MeOH, 60 °C, 24 h) with the addition of the indicated oxidant, bold indicates optimum condition for each parameter, % conversion determined *via* ^1H NMR and is from duplicate experiments (see ESI). Bold indicates the optimum selection

Entry	Oxidant	Eq.	**P1** % conversion
12	—	—	40
15	MnO_2	1.0	25
16	$FeCl_3$	1.0	17
17	$CoCl_2$	1.0	12
18	$NiCl_2$	1.0	2
19	$CuCl_2$	1.0	83
20	$ZnCl_2$	1.0	45
21	$CuSO_4$	1.0	64
22	$Cu(OAc)_2$	1.0	78
23	$CuCl_2$	0.5	61
24	$CuCl_2$	0.25	19

suggesting the Cu^{2+} primarily is responsible for the oxidation with $CuCl_2$ the preferred oxidant (entries 21 and 22, Table 2). Reducing the amount of $CuCl_2$ to 0.5 eq. and 0.25 eq. reduced the conversion to 61% and 19% respectively (entries 23 and 24, Table 2) suggesting a full 1.0 eq. is required for maximum conversion. Copper salts are cheap, easily accessible and their ease of handling and low toxicity profile have found widespread use in organic catalysis. Cu^{2+} mediated aromatisation of cyclohexanone derivatives to phenols,[27] Cu^{2+} catalysed aromatisation of tetrahydrocarbazole to carbazole alkaloids[28] and the synthesis of pyrazoles *via* copper-catalysed relay oxidation have also been reported.[29] In summary, we screen eight transition metal as *in situ* oxidants with Cu^{2+} based oxidants the most significant with $CuCl_2$ providing the best option for *in situ* aromatisation. An LC-MS study was conducted to further examine this synthesis under entry 19 conditions (with $CuCl_2$) to monitor the conversion of **C1** to **P1** *via* the *in situ* **P1*** intermediate (Fig. 3 and Table 3).

After 4.0 hours all chalcone **C1** was consumed with **P1** the major component with detectable **P1***. After 6.0 hours all **P1*** was aromatised to **P1** (Fig. 3 and Table 3). A second LC-MS study was conducted as a negative control using the $NiCl_2$ conditions with contrasting results (Fig. 4 and Table 4).

After 2.0 and 4.0 hours there was still significant **C1** with **P1*** and trace amounts of the desired **P1** present (Fig. 4 and Table 4). Sampling the mixture at 6.0 hrs showed a minor **P1** improvement but with substantial unreacted **C1** still

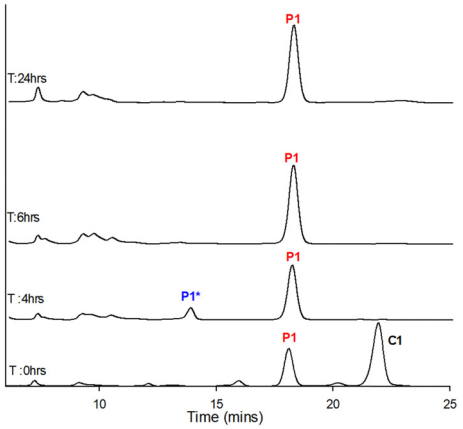

Fig. 3 LC-MS study using entry 19 conditions (Table 2).

Table 3 LC-MS study % conversion using entry 19 conditions from Table 2

Timepoint (h)	**P1*** (%)	**P1** (%)	**C1** (%)
0.0	—	27	57
4.0	4.0	60	2.6
6.0	1	84	—
24.0	—	83	—

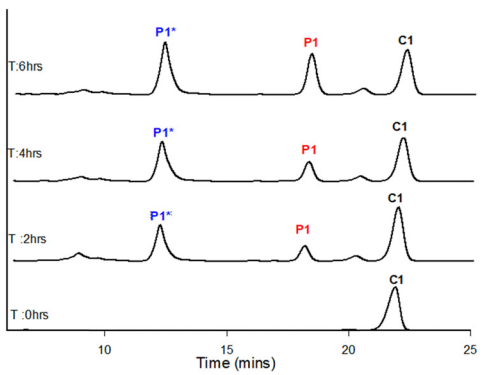

Fig. 4 LC-MS study using entry 18 conditions (Table 2).

Table 4 LC-MS study percentage % conversion using entry 18 conditions

Timepoint (h)	**P1*** (%)	**P1** (%)	**C1** (%)
0.0	—	—	96.0
2.0	18	7.0	62.0
4.0	31.0	11.0	45.0
6.0	36.0	14.0	39

remaining, in contrast to the same timepoint with $CuCl_2$. Further sampling at 8.0 and 24.0 hours failed to show improvement (ESI†) in **P1** demonstrating the choice of transition metal oxidant was critical to the aromatisation process with $CuCl_2$ the superior choice. With a suitable one-pot method to generate

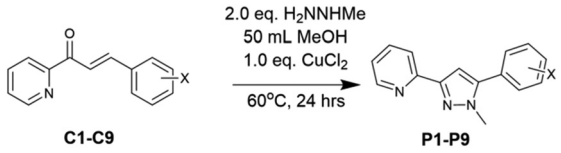

Scheme 4 Synthesis of **P1–P9** using optimised conditions.

pyrazoles selected we validated it by applying it to chalcones with both electron withdrawing and donating aryl units. Chalcones **C1–C9** were prepared *via* literature methods[30] in good to excellent yield (38–92%). The $CuCl_2$ method was applied to **P1** with an isolated yield of 57% which is comparable on the overall yield of 58% over two steps previously reported.[10] This method was also successfully applied to novel pyrazoles **P2–P9** in acceptable yield (38–77%, Scheme 4 and Table 5).

With eight novel potential sensors in hand, we investigated their potential as Zn^{2+} and Cd^{2+} fluorescent sensors in MeCN (Fig. 5), this solvent was selected to allow direct comparison with two previous studies on related pyrazoles.[10,11] Standard protocols for screening fluorescent sensors in organic solvents were followed throughout.[31]

Halogenated pyrazole **P2–P5** all display a "turn on" fluorescent response in the presence of both Zn^{2+} and Cd^{2+} with a higher λ_{em} at 465 nm with Cd^{2+}/Zn^{2+} (Fig. 5). A similar result was observed with the previously reported sensor[11] also displaying λ_{em} at 465 nm with Cd^{2+}/Zn^{2+}. The nature of the electronegative halogen influenced "turn on" intensity when X = 4-F **P2** (Fig. 5A) and 4-Cl **P3** (Fig. 5B) the response is almost identical but as halogen size is increased to 4-Br **P4** (Fig. 5C) and 4-I **P5** (Fig. 5D) the magnitude of λ_{em} is reduced. The halogen series can be summarised as λ_{em} intensity at 465 nm: F $\approx$ Cl > Br < I. These preliminary results suggest the presence of an electronegative group results in a "turn on" response. To test this hypothesis, two additional electronegative pyrazoles were produced pyrazole **P6** bearing a strong electronegative cyano (4-CN) group, which is often compared to F, and a highly electronegative nitro (4-NO_2 group) pyrazole (Fig. 6A and B).

As predicted, pyrazole **P6** with a 4-CN group (Fig. 6A) did display a "turn on" response with both Cd^{2+} and Zn^{2+} analogous to the halogenated pyrazoles **P2–P5** however with reduced intensity at λ_{em} 460 nm. Comparing **P6** directly with **P2**, both of which have similar electronegative withdrawing groups, demonstrates that F is the preferred substituent, and that electronegativity alone is not solely responsible for the "turn on" response. This is further confirmed for **P7** with a NO_2 group displaying "turn on" properties in the presence of Zn^{2+} and Cd^{2+} (Fig. 6B) but with λ_{em} 350 nm in contrast to λ_{em} 460 nm observed in **P2–P6** and **P8**. This indicates the 4-NO_2 group is exerting a significant influence on the photophysical properties of this sensor. An interesting observation was the presence of the electron donating 4-OMe group in **P8** resulted in a minor "turn off" response with both Zn^{2+} and Cd^{2+} (Fig. 6C). A further electron donating pyrazole bearing a 3, 4-Dimethyloxyl group **P9** was synthesized, this followed the trend of **P8** displaying minor "turn off" response in the presence of Zn^{2+} and Cd^{2+} (Fig. 6D). In summary this preliminary screen of eight novel pyrazoles suggests the presence of electron withdrawing groups at the 4-position of the aryl ring result in a "turn on" response in the presence of Zn^{2+} and Cd^{2+} with the chemistry of the group influencing photophysical properties. Electron donating groups on the aryl ring result in a minor "turn off" response also with Zn^{2+} and Cd^{2+}. "Turn on"

Table 5 Chemical yields for **P1–P9** using $CuCl_2$ as an *in situ* oxidant

Entry	X	$CuCl_2$ method yield (%)
P1	4-H	57
P2	4-F	77
P3	4-Cl	61
P4	4-Br	40
P5	4-I	32
P6	4-CN	57
P7	4-NO_2	47
P8	4-OMe	48
P9	3,4-OMe	38

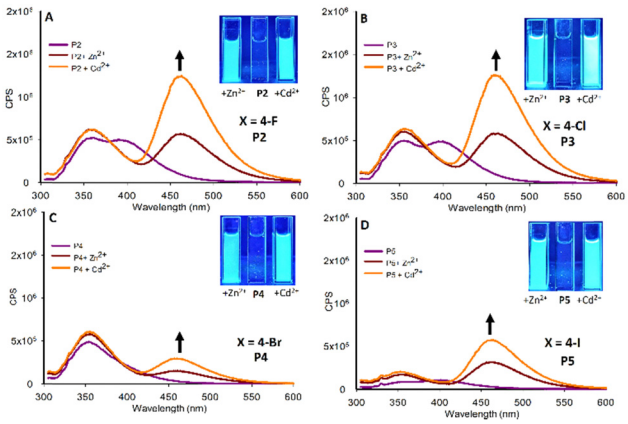

Fig. 5 Fluorescence studies of **P2–P5** (20 μM, MeCN, λ_{ex} 295 nm) with 5.0 eq. Zn^{2+} or Cd^{2+}, insets are pyrazoles at λ_{ex} 365 nm with the indicated metal, cps is counts per second.

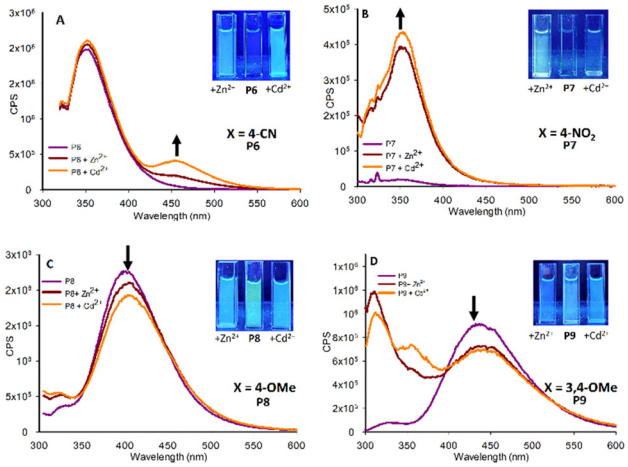

Fig. 6 Fluorescence studies of **P6–P9** (20 μM, MeCN, λ_{ex} 295 nm) with 5.0 eq. Zn^{2+} and Cd^{2+}, insets at λ_{ex} 365 nm with the indicated metals, cps is counts per second.

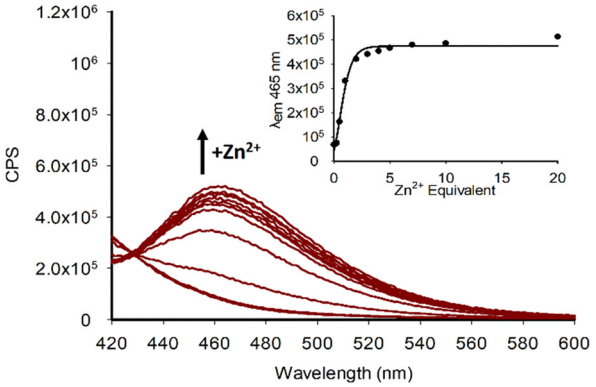

Fig. 7 Fluorescence studies of **P2** (20 μM, MeCN, λ_{ex} 295 nm) with increasing eq. of Zn^{2+} 0.125, 0.25, 0.50, 1.0, 2.0, 3.0, 4.0, 5.0, 7.0, 10.0 and 20.0 eq. Inset is λ_{em} at 465 nm, cps is counts per second.

sensors are typically preferred over "turn off" therefore **P2** was selected for further investigation with Zn^{2+} titration experiments confirming an increased λ_{em} at 465 nm with Zn^{2+} reaching a maximum at 5.0 eq. metal with sensor with further increases in Zn^{2+} resulting in very minor increased fluorescent intensity (Fig. 7).

A similar response was observed with Cd^{2+} however with increased λ_{em} at 465 nm at the same concentration suggesting **P2** would be more suited as a Cd^{2+} sensor (Fig. 8).

The maximum emission was observed at 5.0 eq. Cd^{2+} with further increases resulting in minor increase in emission. A limit of detection (LoD) of 1.97 μM for Zn^{2+} and 0.077 μM for Cd^{2+} was measured for **P2** which is an improvement on the 0.34 μM LoD for **P1** with Cd^{2+} reported previously.[11] A proposed binding mechanism for **P2** with Zn^{2+} is shown in Fig. 9 and agrees with the previously reported crystal structure for **P1** with Zn^{2+}.[11]

A competition assay was performed to assess **P2** λ_{em} in the presence of a range of competing metals (Fig. 10).

Quenching of the "turn on" response was observed with a range of paramagnetic metals including Ni^{2+}, Mn^{2+}, Cu^{2+}, Ru^{3+} and Co^{2+} and this has been observed with similar sensors.[10,11]

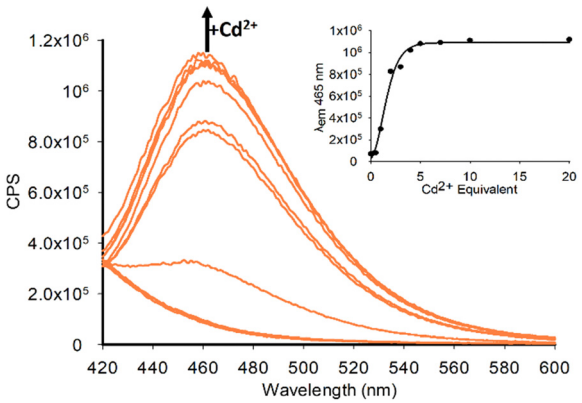

Fig. 8 Fluorescence studies of **P2** (20 μM, MeCN, λ_{ex} 295 nm) with increasing eq. of Cd^{2+} 0.125, 0.25, 0.50, 1.0, 2.0, 3.0, 4.0, 5.0, 7.0, 10.0 and 20.0 eq. Inset is λ_{em} at 465 nm, cps is counts per second.

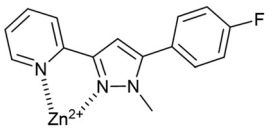

Fig. 9 Proposed binding mechanism of **P2** with Zn^{2+}.

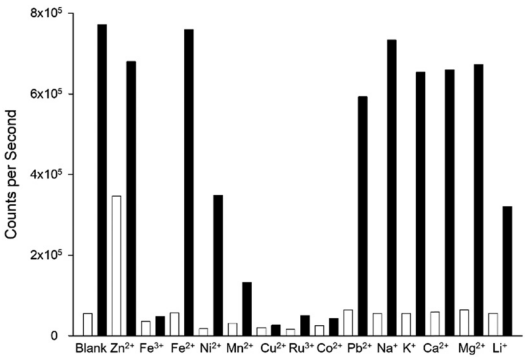

Fig. 10 Competition experiments for **P2**. The white bar represents **P2** (20 μM, MeCN, λ_{ex} 295 nm, λ_{em} 465 nm) with 5.0 eq. of the indicated cation; the black bars is the same with 5.0 eq. Cd^{2+} after equilibrating for 3 min.

Interestingly the presence of diamagnetic metals Zn^{2+} and Pb^{2+} and the group 1 and 2 metals Na^{+}, K^{+}, Ca^{2+} and Mg^{2+} did not result in a significant reduction in λ_{em}. This suggests **P2** could be a useful sensor for the detection of Cd^{2+} in biological samples containing group 1 and 2 metals once a suitable aqueous based derivative of **P2** is developed. The results from the eight novel pyrazoles indicate the 4-position of the aryl ring to be an excellent location for introducing electronegative water solubilising groups to accomplish this. This is the primary focus of the next generation of sensors under development and will be resulted in due course. The one-pot route enables rapid access to novel pyrazoles directly from chalcones greatly accelerating future pyrazole sensors development alongside expediting pyrazole-based molecules with a diverse and wide range of valuable applications.[32]

Conclusions

A new one pot method to synthesize pyrazoles directly from chalcones was developed using $CuCl_2$ as an *in situ* oxidant which was validated against a range of electron donating and withdrawing chalcones resulting in eight novel pyrazole based sensors. These sensors were confirmed to display both "turn on" and "turn off" properties dependent on aryl ring substitution. The presence of electronegative groups at the 4-position resulted in a "turn on" sensor with the chemistry of the group influencing the extent of λ_{em} wavelength. Electro donating groups displayed a very mild "turn off" response. The 4-position is well suited to a variety of substitution and would be an excellent position for the introduction of water solubilising groups to transition away from a purely organic solvent-

based sensor to an aqueous one, this is an ongoing objective and will be reported shortly. This simple modular scaffold would be highly amenable to a multi-sensor approach incorporating multiple chelation sites with valuable applications in real world monitoring. While the focus of this study was efficient access to pyrazoles for the design screening of sensors, this direct one pot approach also enables efficient access to future pyrazoles with applications in anti-cancer, anti-infective and anti-inflammatory screening studies and will be of benefit to the wider chemistry community.[32]

Author contributions

Alexander Ciupa designed, synthesized, characterised, performed all spectroscopy studies and authored the manuscript.

Data availability

The data supporting this article have been included as part of the ESI.†

Conflicts of interest

There are no conflicts to declare.

Acknowledgements

The author acknowledges Steven Robinson for assistance with time-of-flight high resolution mass spectrometry, Glyn Connolly for NMR spectroscopy guidance and Krzysztof Pawlak with fluorescence spectroscopy. This work made use of shared equipment located at the Materials Innovation Factory; created as part of the UK Research Partnership Innovation Fund (Research England) and co-funded by the Sir Henry Royce Institute.

References

1 Selected examples: (*a*) S. Fustero, M. Sánchez-Roselló, P. Barrio and A. Simón-Fuentes, *Chem. Rev.*, 2011, **111**(11), 6984; (*b*) M.-C. Ríos and J. Portilla, *Chemistry*, 2022, **4**, 940; (*c*) J.-C. Castillo and J. Portilla, *Targets Heterocycl. Syst.*, 2018, **22**, 194.
2 R. F. Costa, L. C. Turones, K. V. N. Cavalcante, I. A. Rosa Júnior, C. H. Xavier, L. P. Rosseto, H. B. Napolitano, P. F. S. Da Castro, M. L. F. Neto, G. M. Galvão, R. Menegatti, G. R. Pedrino, E. A. Costa, J. L. R. Martins and J. O. Fajemiroye, *Front. Pharmacol.*, 2021, **12**, 666725.
3 A. T. Taher, M. T. Mostafa Sarg, N. R. El-Sayed Ali and N. Hilmy Elnagdi, *Bioorg. Chem.*, 2019, **89**, 103023.
4 B. Insuasty, A. Tigreros, F. Orozco, J. Quiroga, R. Abonía, M. Nogueras, A. Sanchez and J. Cobo, *Bioorg. Med. Chem.*, 2010, **18**, 4965.
5 J. V. Faria, P. F. Vegi, A. G. C. Miguita, M. S. Dos Santos, N. Boechat and A. M. R. Bernardino, *Bioorg. Med. Chem.*, 2017, **25**, 5891.
6 Selected examples: (*a*) B. Willy and T. J. Mueller, *Eur. J. Org. Chem.*, 2008, 4157; (*b*) V. Mukundam, S. Sa, A. Kumari, R. Das and K. Venkatasubbaiah, *J. Mater. Chem. C*, 2019, **7**, 12725; (*c*) A. C. Murali, P. Pratakshya, P. Patel, P. Nayak, S. Peruncheralathan and K. Venkatasubbaiah, *New J. Chem.*, 2023, **47**, 17835; (*d*) S. Mukherjee, P. S. Srinivasan and S. Peruncheralathan, *Chem. Commun.*, 2015, **51**, 17148.
7 Selected examples: (*a*) A. Tigreros and J. Portilla, *Curr. Chin. Sci.*, 2021, **1**, 197; (*b*) A. Tigreros and J. Portilla, *RSC Adv.*, 2020, **10**, 19693; (*c*) M. Verma, A. F. Chaudhry, M. T. Morgan and C. J. Fahmi, *Org. Biomol. Chem.*, 2010, **8**, 363.
8 S. Sa, V. Mukundam, A. Kumari, R. Das and K. Venkatasubbaiah, *Dalton Trans.*, 2021, **50**, 6204.
9 Y.-Q. Gu, W.-Y. Shen, Y. Mi, Y.-F. Jing, J.-M. Yuan, P. Yu, W.-M. Zhu and F.-L. Hu, *RSC Adv.*, 2019, **9**, 35671.
10 A. Ciupa, *RSC Adv.*, 2024, **14**, 3519.
11 A. Ciupa, M. F. Mahon, P. A. De Bank and L. Caggiano, *Org. Biomol. Chem.*, 2012, **10**, 8753.
12 T. V. O'Halloran, *Science*, 1993, **261**, 715.
13 C. Andreini and I. Bertini, *J. Inorg. Biochem.*, 2012, **111**, 150.
14 C. J. Frederickson, *Biometals*, 2001, **14**, 353.
15 G. Genchi, S. M. Sinicropi, G. Lauria, A. Carocci and A. Catalano, *Int. J. Environ. Res. Public Health*, 2020, **17**, 3782.
16 P. Singh, A. Anand and V. Kumar, *Eur. J. Med. Chem.*, 2014, **85**, 758.
17 Selected examples: (*a*) A. Ciupa, N. J. Griffiths, S. K. Light, P. J. Wood and L. Caggiano, *Med. Chem. Commun.*, 2011, **2**, 1011; (*b*) M. A. Shalaby, S. A. Rizk and A. M. Fahim, *Org. Biomol. Chem.*, 2023, **21**, 5317; (*c*) A. Gupta, S. Garg and H. Singh, *Anal. Methods*, 2020, **12**, 5022; (*d*) S. Wangngae, T. Pewklang, K. Chansaenpak, P. Ganta, S. Worakaensai, K. Siwawannapong, S. Kluaiphanngam, N. Nantapong, R.-Y. Lai and A. Kamkaew, *New J. Chem.*, 2021, **45**, 11566; (*e*) A. Ahmad, M. Y. Wani, M. Patel, A. J. F. N. Sobral, A. G. Duse, F. M. Aqlan and A. S. Al-Bogami, *Med. Chem. Commun.*, 2017, **8**, 2195.
18 Selected examples: (*a*) G. Cocconcelli, E. Diodato, A. Caricasole, G. Gaviraghi, E. Genesio, C. Ghiron, L. Magnoni, E. Pecchioli, R. V. Plazzi and G. C. Terstappen, *Bioorg. Med. Chem.*, 2008, **16**, 2043; (*b*) A. Voskiene, V. Mickevicius and G. Mikulskiene, *ARKIVOC*, 2007, 303; (*c*) S. B. Somappa, J. S. Biradar, P. Rajesab, S. Rahber and M. Sundar, *Monatsh. Chem.*, 2015, **146**, 2067.
19 Selected examples: (*a*) H. Zhang, Q. Wei, G. Zhu, J. Qu and B. Wang, *Tetrahedron Lett.*, 2016, **57**, 2633; (*b*) S. M. Landge, A. Schmidt, V. Outerbridge and B. Török, *Synlett*, 2007, 1600.
20 A. Ciupa, P. A. De Bank, M. F. Mahon, P. J. Wood and L. Caggiano, *MedChemComm*, 2013, **4**, 956.
21 B. Varghese, S. N. Al-Busa, F. O. Suliman and S. M. Z. Al-Kindy, *RSC Adv.*, 2017, **7**, 46999.
22 I. Bhatnagar and M. V. George, *Tetrahedron*, 1968, **24**, 1293.
23 G. S. Ananthnag, A. Adhikari and M. S. Balakrishna, *Catal. Commun.*, 2014, **43**, 240.
24 J. N. Shah and C. K. Shah, *J. Org. Chem.*, 1978, **43**(6), 1266.

25 Selected examples: (*a*) P. D. Lokhande, B. A. Dalvi, V. T. Humne, B. R. Nawghare and A. Kareem, *Ind. J. Chem.*, 2014, **53B**, 1091; V. K. Rao, R. Tiwari, B. S. Chhikara, A. N. Shirazi, K. Parang and A. Kumar, *RSC Adv.*, 2013, **3**, 15396.

26 Selected examples: (*a*) R. A. Sheldon, *Chem. Soc. Rev.*, 2012, **41**, 1437–1451; (*b*) R. A. Sheldon, *Chem. Commun.*, 2008, 3352.

27 Selected examples: (*a*) X. Liu, J. Chen and T. Ma, *Org. Biomol. Chem.*, 2018, **16**, 8662–8676; (*b*) X.-L. Liu, X.-L. Long, Y.-J. Guo, C.-H. Meng, A.-B. Xia and D.-Q. Xu, *Asian J. Org. Chem.*, 2017, **6**, 967; (*c*) H.-C. Tong, R. Reddy and S.-T. Liu, *Eur. J. Org. Chem.*, 2014, 3256.

28 B. A. Dalvi and P. D. Lokhande, *Tetrahedron Lett.*, 2018, **59**, 2145.

29 X. Tang, L. Huang, J. Yang, Y. Xu, W. Wu and H. Jiang, *Chem. Commun.*, 2014, **50**, 14793.

30 Selected examples: (*a*) H. M. Faidallah, M. M. Al-Mohammadi, K. A. Alamry and K. A. Khan, *J. Enzyme Inhib. Med. Chem.*, 2016, **31**(S1), 1570163; (*b*) J. Majeed and M. Shaharyar, *J. Enzyme Inhib. Med. Chem.*, 2011, **26**(6), 819; (*c*) Y.-J. Ren, Z.-C. Wang, X. Zhang, H.-Y. Qiu, P.-F. Wang, H.-B. Gong, A.-Q. Jiang and H.-L. Zhu, *RSC Adv.*, 2015, **5**, 21445.

31 Selected examples: (*a*) S. Lohar, S. Pal, M. Mukherjee, A. Maji, N. Demitri and P. Chattopadhyay, *RSC Adv.*, 2017, **7**, 25528; (*b*) M. Akula, P. Z. El-Khoury, A. Nag and A. Bhattacharya, *RSC Adv.*, 2014, **4**, 25605; (*c*) Z. Shi, Y. Tu and S. Pu, *RSC Adv.*, 2018, **8**, 6727; (*d*) Y. Zhang, H. Lui, W. Gao and S. Pu, *RSC Adv.*, 2019, **9**, 27476; (*e*) X. Wu, Z. Zhang, H. Liu and S. Pu, *RSC Adv.*, 2020, **10**, 15547.

32 A. Ansari, A. Abi, M. Asif and S. Shamsuzzaman, *New J. Chem.*, 2017, **41**, 16.

